Formation of toroidal Li_2O_2 in non-aqueous Li-O_2 batteries with Mo_2CT_x MXene/CNT composite

Mihye Wu[a,b], Do Youb Kim[b,d], Hyunsoo Park[a], Kyeong Min Cho[a], Ju Ye Kim[a], Seon Joon Kim[c], Sungho Choi[b], Yongku Kang[b,d], Jihan Kim[a]*, Hee-Tae Jung[a]*

[a]Department of Chemical and Biomolecular Engineering (BK-21 Plus), KAIST Institute for Nanocentury, Korea Advanced Institute of Science and Technology, 291 Daehak-ro, Yuseong-gu, Daejeon 34141, Republic of Korea

[b]Advanced Materials Division, Korea Research Institute of Chemical Technology, Yuseong-gu, Daejeon 34114, Korea

[c]Materials Architecturing Research Center, Korea Institute of Science and Technology (KIST), Seoul 02792, Republic of Korea

[d]Department of Chemical Convergence Materials, Korea University of Science and Technology (UST), Yuseong-gu, Dajeon 34113, Korea

*Corresponding authors

Jihan Kim, +81-42-350-7311, Fax: +82-42-350-3910, E-mail: jihankim@kaist.ac.kr

Hee-tae Jung Tel: +82-42-350-3931, Fax: +82-42-350-8452, E-mail: heetae@kaist.ac.kr

KEYWORDS Mo_2CT_x, MXene, toroidal Li_2O_2, O_2 adsorbability, solution growth model, Li-O_2 battery

Table S1. BET surface area of the CNT and CNT/Mo_2CT_x electrode

CNT (m^2/g)	**CNT/Mo_2CT_x (m^2/g)**
172.6	134.9

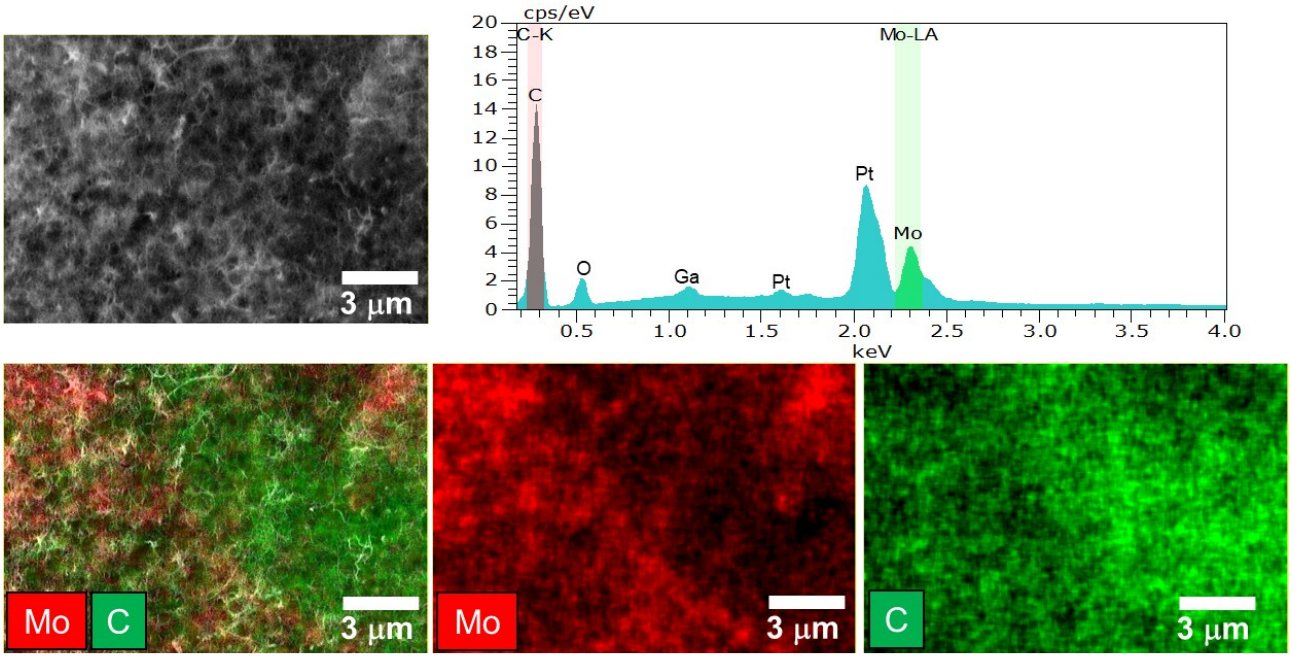

Figure S1. EDS mapping of the CNT/Mo_2CT_x electrode

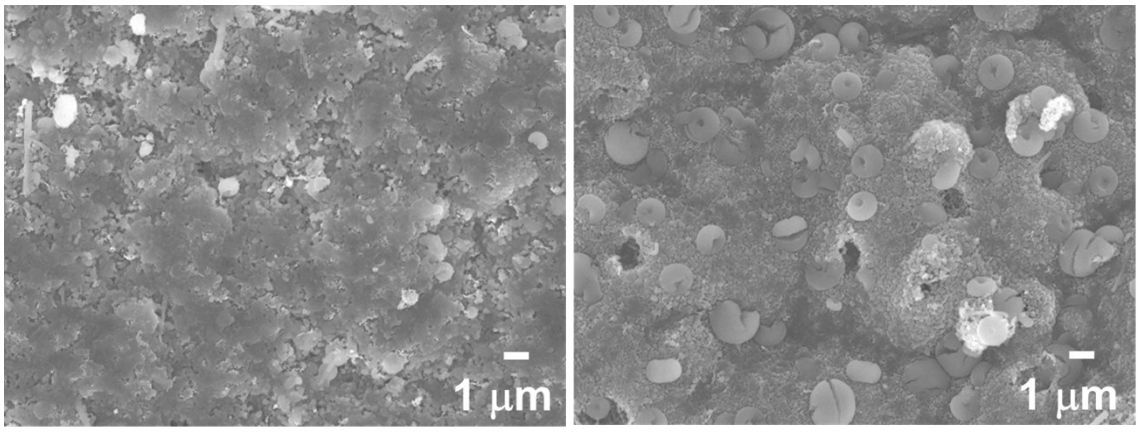

Figure S2. *Ex situ* SEM images of the CNT electrode

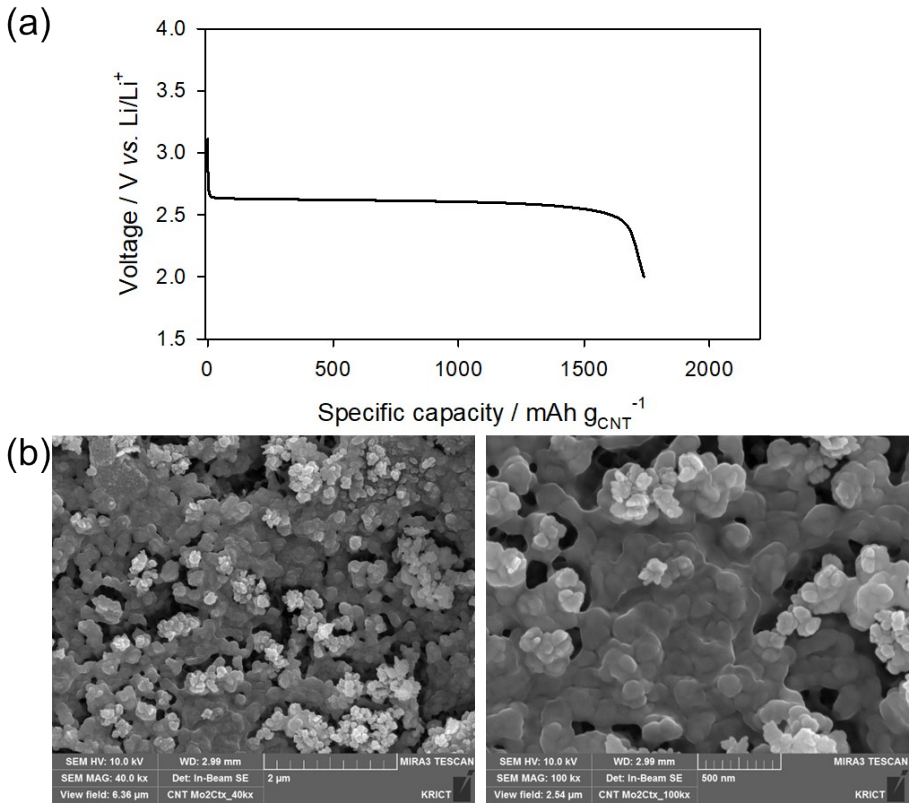

Figure S3. (a) Discharge capacity (b) *Ex situ* SEM images of the CNT/Mo_2CT_x electrode discharged under 1 M LiTFSI in TEGDME

Section 1. Vibrational Frequency Analysis

Phonon dispersion spectra were calculated using the PHONOPY code with 4 X 4 X 1 supercell. It provides the information for the dynamical stability of geometry optimized structures based on density functional perturbation theory.

There is the phonon dispersion spectrum of geometry optimized Mo_2C using PBE-D3 in Figure S1a. It indicates that there is no imaginary frequency in the high symmetry k-path. However, all models of $Mo_2C(OH)_2$ have some imaginary frequencies. These tendencies are also found in α-Mo_2C by B. I. Yakobson et al.[2] They claimed that the calculated phonon dispersion of the various models for α-$Mo_2C^{(OH)_2}$ have imaginary frequencies around the M points while α-Mo2C don't have the imaginary frequencies in high symmetry k-path. So, α-$Mo_2C^{(OH)_2}$ is regarded as being structurally unstable. This would indicate that all the models in this paper are β-Mo_2C, but it has same tendency with α-Mo_2C. Although $Mo_2C^{(OH)_2}$ have some dynamical instability, the model 3 of $Mo_2C^{(OH)_2}$, which is the most stable model, was selected in order to calculate the interaction of O_2 adsorption. Because model 3 has only small imaginary frequencies around the Γ and M point as well as the lowest energy when comparing mode 1 and 2.

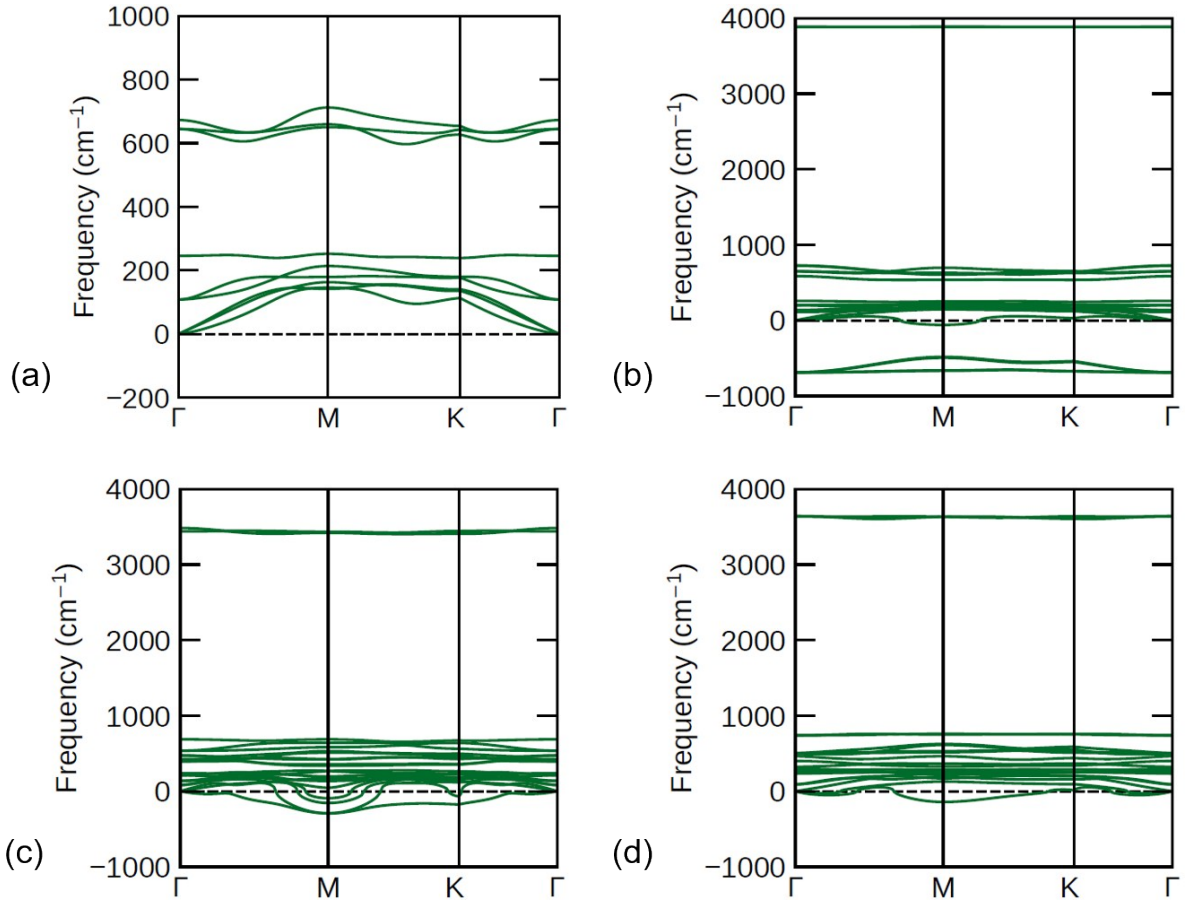

Figure S4. There are phonon dispersion spectrum calculated by the PHONOPY code with 4 X 4 X 1 supercell: (a)^{Mo_2C}, (b) the model 1 of $^{Mo_2C(OH)_2}$, (c) the model 2 of $^{Mo_2C(OH)_2}$, (d) the model 3 of $^{Mo_2C(OH)_2}$.

Section 2. Crystal structures

1. Mo_2C

```
data_Opt_Mo2C
_symmetry_space_group_name_H-M       'P1'
_symmetry_Int_Tables_number          1
_symmetry_cell_setting               triclinic
loop_
_symmetry_equiv_pos_as_xyz
   x,y,z
_cell_length_a                       2.9649
_cell_length_b                       2.9649
_cell_length_c                       32.3383
_cell_angle_alpha                    90.0000
_cell_angle_beta                     90.0000
_cell_angle_gamma                    120.0000
loop_
_atom_site_label
_atom_site_type_symbol
_atom_site_fract_x
_atom_site_fract_y
_atom_site_fract_z
_atom_site_U_iso_or_equiv
Mo1     Mo     0.66667     0.33333     0.46310     0.00000
Mo2     Mo     0.33333     0.66667     0.53690     0.00000
C3      C      0.00000     0.00000     0.50000     0.00000
```

2. Model 1 of $Mo_2C(OH)_2$

data_Opt_model1
_symmetry_space_group_name_H-M 'P1'
_symmetry_Int_Tables_number 1
_symmetry_cell_setting triclinic
loop_
_symmetry_equiv_pos_as_xyz
x,y,z
_cell_length_a 3.0901
_cell_length_b 3.0901
_cell_length_c 29.7716
_cell_angle_alpha 90.0000
_cell_angle_beta 90.0000
_cell_angle_gamma 120.0000
loop_
_atom_site_label
_atom_site_type_symbol
_atom_site_fract_x
_atom_site_fract_y
_atom_site_fract_z
_atom_site_U_iso_or_equiv

Mo1	Mo	0.66667	0.33333	0.46155	0.00000
Mo2	Mo	0.33333	0.66667	0.53845	0.00000
H3	H	0.33333	0.66667	0.63442	0.00000
O4	O	0.33333	0.66667	0.60213	0.00000
H5	H	0.66667	0.33333	0.36558	0.00000
O6	O	0.66667	0.33333	0.39787	0.00000
C7	C	0.00000	0.00000	0.50000	0.00000

3. Model 2 of $Mo_2C(OH)_2$

data_Opt_model2

_symmetry_space_group_name_H-M 'P1'
_symmetry_Int_Tables_number 1
_symmetry_cell_setting triclinic
loop_
_symmetry_equiv_pos_as_xyz
x,y,z
_cell_length_a 2.9726
_cell_length_b 2.9726
_cell_length_c 32.1711
_cell_angle_alpha 90.0000
_cell_angle_beta 90.0000
_cell_angle_gamma 120.0000
loop_
_atom_site_label
_atom_site_type_symbol
_atom_site_fract_x
_atom_site_fract_y
_atom_site_fract_z
_atom_site_U_iso_or_equiv

Mo1	Mo	0.66667	0.33333	0.46130	0.00000
Mo2	Mo	0.33333	0.66667	0.53870	0.00000
H3	H	-0.00000	0.00000	0.38655	0.00000
O4	O	-0.00000	0.00000	0.58293	0.00000
H5	H	0.00000	-0.00000	0.61345	0.00000
O6	O	0.00000	-0.00000	0.41707	0.00000
C7	C	0.00000	0.00000	0.50000	0.00000

4. Model 3 of $Mo_2C(OH)_2$

data_Opt_model3

_symmetry_space_group_name_H-M 'P1'
_symmetry_Int_Tables_number 1
_symmetry_cell_setting triclinic
loop_
_symmetry_equiv_pos_as_xyz
x,y,z
_cell_length_a 3.2688
_cell_length_b 3.2688
_cell_length_c 26.6047
_cell_angle_alpha 90.0000
_cell_angle_beta 90.0000
_cell_angle_gamma 120.0000
loop_
_atom_site_label
_atom_site_type_symbol
_atom_site_fract_x
_atom_site_fract_y
_atom_site_fract_z
_atom_site_U_iso_or_equiv

Mo1	Mo	0.66667	0.33333	0.46424	0.00000
Mo2	Mo	0.33333	0.66667	0.53576	0.00000
O3	O	0.66667	0.33333	0.58526	0.00000
O4	O	0.33333	0.66667	0.41474	0.00000
H5	H	0.33333	0.66667	0.37811	0.00000
H6	H	0.66667	0.33333	0.62189	0.00000
C7	C	0.00000	0.00000	0.50000	0.00000